Expanding the Enzymatic Polymerization Landscape by Lipid Mesophase Soft Nanoconfinement

Patrick Züblin, Adrian Zeller, Claire Moulis, Magali Remaud-Simeon, Yang Yao, Raffaele Mezzenga

GDCh

Research Articles

Angewandte
Chemie
International Edition
www.angewandte.org

Enzyme Immobilization | Hot Paper

Expanding the Enzymatic Polymerization Landscape by Lipid Mesophase Soft Nanoconfinement

Patrick Züblin, Adrian Zeller, Claire Moulis, Magali Remaud-Simeon, Yang Yao, and
Raffaele Mezzenga*

Abstract: Soft nanoconfinement can increase chemical reactivity in nature and has therefore led to considerable interest in transferring this universal feature to artificial biological systems. However, little is known about the underlying principles of soft nanoconfinement responsible for the enhancement of biochemical reactions. Herein we demonstrate how enzymatic polymerization can be expanded, optimized, and engineered when carried out under soft nanoconfinement mediated by lipidic mesophases. By systematically varying the water content in the mesophase and thus the diameter of the confined water nanochannels, we show higher efficiency, turnover rate, and degrees of polymerization as compared to the bulk aqueous solution, all controlled by soft nanoconfinement effects. Furthermore, we exploit the unique properties of unfreezing soft nanoconfined water to perform the first enzymatic polymerization at −20 °C in pure aqueous media. These results underpin lipidic mesophases as a versatile host system for chemical reactions and promote them as an original and unexplored platform for enzymatic polymerization.

Introduction

Confinement may have played an instrumental role in the origin of life[1,2] and remains a ubiquitous requirement of modern life, where compartmentalization of cells enables the efficient synthesis of biomolecules.[3] Nearly all relevant reactions in biological systems are catalyzed by enzymes,[4] many of which occur in a confined environment.[5–8] Accord-

[*] P. Züblin, A. Zeller, Dr. Y. Yao, Prof. Dr. R. Mezzenga
Department of Health Sciences and Technology, ETH Zürich
Schmelzbergstrasse 9, 8092 Zürich (Switzerland)
E-mail: raffaele.mezzenga@hest.ethz.ch

Dr. C. Moulis, Prof. Dr. M. Remaud-Simeon
TBI, Université de Toulouse, CNRS, INRAE, INSA
135 Av. de Rangueil, 31400 Toulouse (France)

Prof. Dr. R. Mezzenga
Department of Materials, ETH Zürich
Wolfgang-Pauli-Strasse 10, 8093 Zürich (Switzerland)

ingly, the performance of enzymes under confinement ought to be profoundly different than in bulk aqueous solution, which is normally used to study the catalytic properties of enzymes.[9,10] Different artificial soft nanoconfined systems, such as reversed micelles, liposomes, or water-in-oil microemulsions,[11–15] have demonstrated that nanoconfined enzymatic reactions can outperform their homologue reactions in bulk solution. However, explanations for the effect of nanoconfinement still remain elusive, and studies on soft nanoconfined enzymatic reactions are scarce.[9,16] Consequently, as we endeavor to mimic the superior chemical reactivity observed in nature, a better understanding of the impact of soft nanoconfinement on fundamental biochemical reactions, such as enzymatic polymerization,[17] is imperative.

Lipidic mesophases offer an excellent opportunity to explore the effect of soft nanoconfinement on enzymatic reactions. They are formed in a self-assembly process when certain readily accessible lipids are mixed with water, resulting in a rich polymorphism of well-studied mesophase symmetries.[18,19] Specifically, the bicontinuous cubic *Ia3d* and *Pn3m* phases, which are characterized by a network of water channels separated by lipid bilayers with high interfacial area, allow for soft confinement of enzymes in a biomimetic environment.[20,21] Over the past decade, a number of studies have incorporated enzymes into lipidic mesophases while maintaining the mesophase structure.[22–29] Enzymatic synthesis reactions have been successfully implemented in lipidic mesophase (in meso), with threefold increased efficiency in the synthesis of a carbohydrate[30] or enhanced chirality of the product as compared to that in bulk solution.[31] Using non-freezing lipids, it was recently shown that lipidic mesophases can prevent water from crystallizing down to −120 °C, allowing expanding the study of enzymatic reactions in liquid water at subzero temperatures.[32–34] While work in this area is still in its infancy, this opens up intriguing possibilities to unravel the diversity of life thriving in cryogenic conditions.[35]

Herein we report the first enzymatic polymerization conducted in lipidic mesophases. By performing the enzymatic synthesis of the polymer dextran (Figure 1a) as a model reaction in the mesophase, we found a sixfold increase in polymer polymerization degree coupled with a faster yield when the synthesis was carried out in meso as compared to the homologue reaction in bulk solution. In addition, we observed a systematic change in polymer molecular weight when we adjusted the hydration level of the mesophase, which can be ascribed solely to the confinement effect. Finally, we were able to enzymatically synthe-
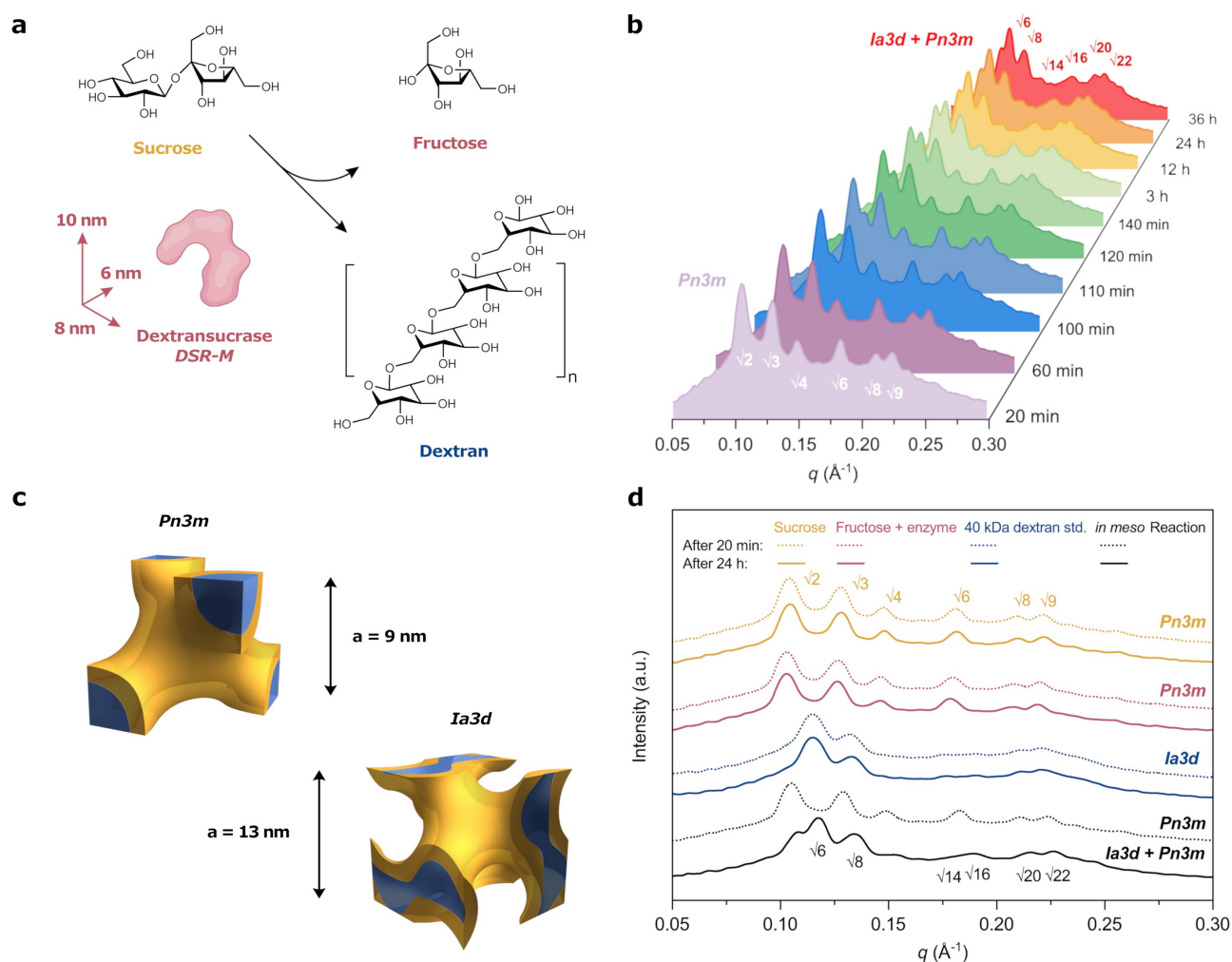
Figure 1. Mesophase structure during enzymatic dextran synthesis. a) Enzymatic synthesis of dextran. The approximate size of the enzyme dextransucrase *DSR-M* is indicated. b) Representative in situ SAXS profiles of dextran synthesis in the mesophase over 36 h. c) Illustrations of the repeating units of the bicontinuous cubic *Pn3m* and *Ia3d* phases. The lipid bilayer is shown in yellow, and one of the two water channel networks is shown in blue. The lattice parameter *a* is added as determined by SAXS. d) SAXS profiles of M70-B30 in the presence of the individual reaction compounds presented in (a). All compounds were dissolved in the buffer part of the mesophase. In addition, in meso reaction data from (b) for 20 min and 24 h are included. The relative *q*-values of the Bragg peak positions are included in the SAXS profiles. Synthesis conditions: 70 wt% monolinolein and 30 wt% buffer (M70-B30) containing 50 mg/mL sucrose and 1 U/mL enzyme at 30 °C. *q*, modulus of scattering vector; std., standard; a.u., arbitrary units.

size dextran under cryogenic conditions by running the reaction in meso, which, to our knowledge, represents the first enzymatic polymerization in pure liquid aqueous media at −20 °C. Our results highlight the versatility of lipidic mesophases as a platform for enzymatic polymerization, providing keys to the understanding of soft nanoconfinement effects with far-reaching implications spanning from nanotechnology to the foundations of biology.

Results and Discussion

Synthesis conditions and approach

To investigate the effect of soft nanoconfinement on the enzymatic synthesis of dextran, we chose a composition of

70 wt% monolinolein and 30 wt% aqueous phase (buffer solution), which gives rise to the *Pn3m* symmetry based on the established phase diagram of monolinolein and pure water.[19] The *Pn3m* symmetry offers promising synthesis conditions as it has the highest level of hydration at ambient conditions without entering the excess water regime,[21] that is, providing a tunable nanoconfinement. We used the recombinant dextransucrase *DSR-M* from *Leuconostoc citreum* NRRL B-1299, which exclusively produces short, linear dextran polymers in bulk solution,[36] allowing the detection of subtle differences in the biochemical behavior of the enzyme by high-performance size exclusion chromatography (HPSEC) when immobilized in meso. By keeping the synthesis conditions in the aqueous part of the mesophase and in the bulk solution identical, i.e., 50 mg/mL sucrose and 1 U/mL enzyme at 30 °C, we ensured an

unambiguous comparison of the reaction in the two systems solely in terms of the lipidic mesophase nanoconfinement.

Characterization of the lipid mesophase during in meso dextran synthesis

The mesophase symmetry during the enzymatic synthesis of dextran was monitored using small-angle X-ray scattering (SAXS). After a slight shift of the peak position towards higher q-values up to 80 min, a phase transition from the double diamond $Pn3m$ into a mixed $Ia3d+Pn3m$ cubic phase was observed (Figure 1b, 1c and S1). The cubic phase was maintained for up to 36 h, with no change in the SAXS pattern between 12 and 36 h, which demonstrated the successful incorporation of all the reactants for an enzymatic polymerization into the mesophase. An average lattice parameter of 9 and 13 nm was calculated for the $Pn3m$ and $Ia3d$ symmetries, respectively, while the water channel diameter was calculated to be 3 nm for the $Pn3m$ and assumed to remain approximately constant in the $Ia3d+Pn3m$ coexistence regime.[37] Therefore, we expected the *DSR-M* enzyme to be immobilized and partitioned between individual, partially bent bilayers of the mesophase[30] given that its size is approximately represented by a cuboid of $6\times8\times10$ nm.[36]

To decipher the observed phase transition in terms of the individual effects of reactant, enzyme, and products on the symmetry, we prepared three identical mesophases, separately loaded by the reaction ingredients and products at concentrations matching complete conversion under the chosen synthesis conditions. The SAXS profiles showed that the $Pn3m$ symmetry was not altered by the presence of sucrose, fructose, or the enzyme over time (Figure 1d). However, in the presence of a 40 kDa dextran standard, the symmetry changed to the Ia3d cubic phase. The appearance of the $Ia3d$ phase can be explained by the water-binding capacity of dextran[38] in combination with size-related configurational changes of the macromolecular chains of dextran. The phase diagram of monolinolein and pure water[19] shows an isothermal transition from $Pn3m$ to $Ia3d$ as the water content is decreased. Recently, it has been shown that confined water in lipidic cubic phases exists in two dynamically different states: water bound to the lipid headgroups and interstitial free water.[39] Thus, when dextran polymers with end-to-end distances exceeding the water channel diameter are introduced into the mesophase, they first need to change their conformation within the mesophase to remain within the water nanochannels, promoting order-order transitions[37] and additionally reducing the water available for hydration of the lipid headgroups; both effects are believed to contribute to the transition to the $Ia3d$ phase, which normally exists at a lower water content. This is consistent with the observed transition $Pn3m\rightarrow Ia3d+Pn3m$ during the synthesis of 49 kDa dextran. It should be noted that the consumption of water molecules for dextran synthesis is insignificant compared to the amount of water present under our synthesis conditions. Indeed, sucrose hydrolysis (without chain elongation) is a minor reaction

occurring only during the initial phase of the reaction to produce glucose used, with sucrose itself, as a chain initiator, followed by the second major phase of chain elongation.[36] As a consequence, water consumption has no effect on the mesophase structure. Interestingly, the order-order transition from $Pn3m$ to $Ia3d+Pn3m$ is itself an indirect indication that polymerization is happening. Indeed, we know that a $Pn3m$ phase at 30 % water will shift to an $Ia3d$ phase when a 40 kDa dextran is added (40 kDa dextran being an imposed endpoint of the reaction). Similarly, at the same water content, which was selected for favorable synthesis conditions, we observe a transition from $Pn3m$ to $Ia3d+Pn3m$ during polymerization.

Comparison of dextran synthesis between in meso and bulk solution

The effect of lipidic mesophase nanoconfinement on enzymatic polymerization was evaluated by monitoring the enzymatic synthesis of dextran in meso and comparing it with that carried out in bulk solution. First, we collected molecular weight (M_w) and dispersity ($Đ$) data of synthesized dextran using HPSEC. When the polymerization was conducted in meso, we observed a remarkable increase in the final molecular weight of the synthesized dextran ($M_w =$ 49 kDa) by more than sixfold after 24 h compared to the reaction in bulk solution ($M_w = 8$ kDa) (Figure 2a and 2b). After 24 h, no further activity was detected in either the mesophase or the bulk solution (Figure S2). In addition, a pronounced difference in the evolution of M_w can be seen, with M_w in the bulk solution rising from 4 kDa to 8 kDa between 1 and 24 h, whereas in the mesophase, a M_w of around 50–60 kDa coupled with high $Đ$ values (≈ 2) was already detected in the first 30 min of the reaction. For the initial 1 h reaction in bulk solution, we were unable to extract values for M_w and $Đ$, as the amount of synthesized dextran was below the limit of detection. The in meso synthesized dextran showed a broader dispersity after 24 h ($Đ = 1.7$) compared to that in bulk solution ($Đ = 1.1$ after 24 h), which we believe is explained by nanoconfinement-induced concentration gradients of sucrose and oligosaccharides, both acting as substrates for chain elongation, in confined water,[39,40] but also by the larger molecular weight achieved. The above findings obtained by HPSEC suggest a fundamental difference in the working mechanism of the enzyme, with a significantly higher efficiency in polymer chain elongation when immobilized in the mesophase.

We next examined the yield over time of dextran synthesized in meso and in bulk solution based on the starting concentration of sucrose. For this purpose, synthesized dextran was purified and hydrolyzed, and free glucose was quantified by high-performance anion exchange chromatography (HPAEC). The in meso reaction yielded approximately twice as much dextran in the first 2–3 h of the reaction compared to the reaction in bulk solution, indicating a higher turnover rate of the immobilized enzyme (Figure 2c). This result agrees well with the larger peak areas of the molecular weight distribution curves of the in
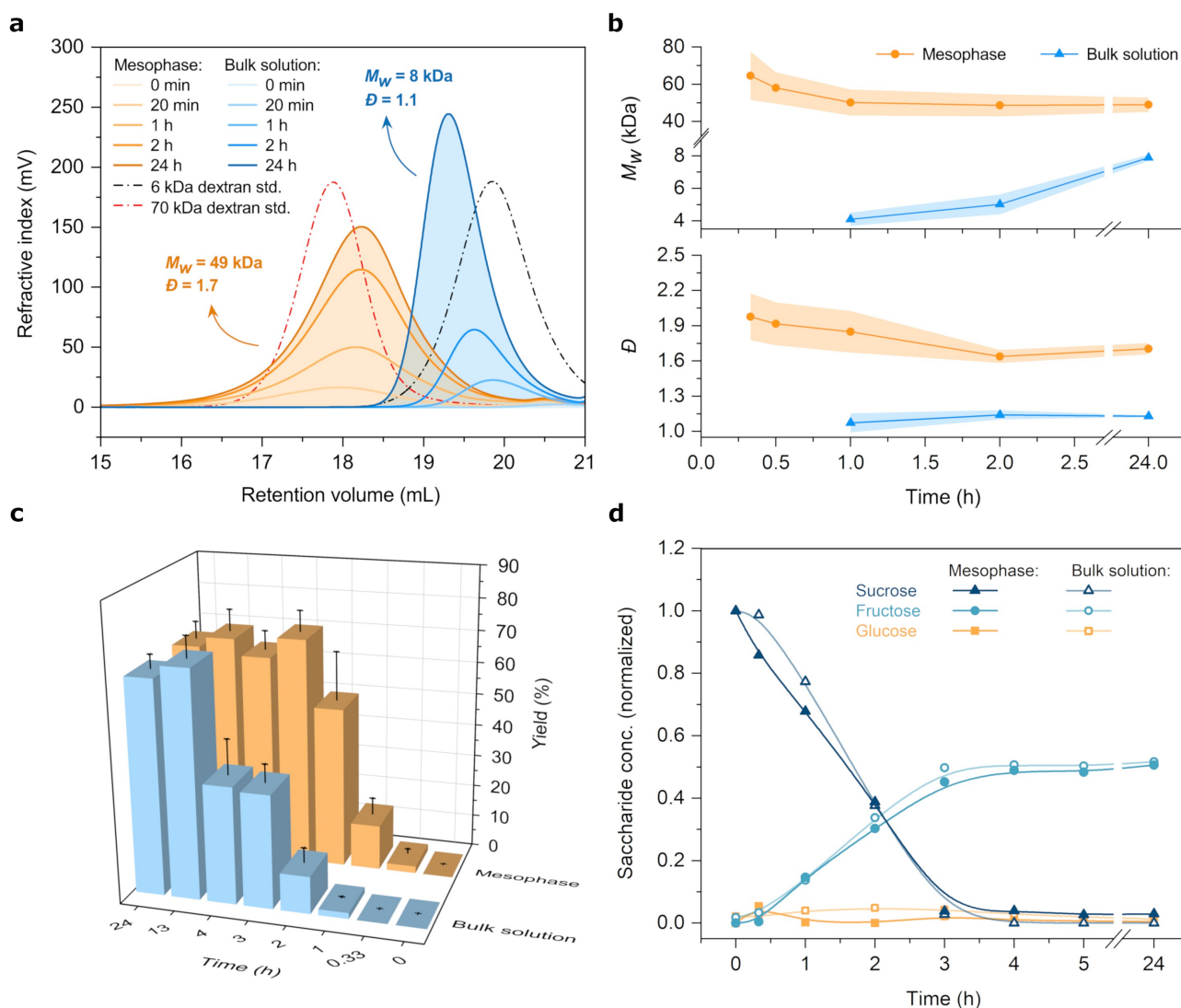
Figure 2. Comparison of dextran synthesis performed in meso and in bulk solution. a, b) Representative HPSEC profiles of dextran synthesized in meso and in bulk solution (a) and corresponding monitoring of molecular weight (M_w) and dispersity ($Đ$) (b). HPSEC profiles of commercial dextran standards (std., 6 and 70 kDa) are included as visual references in (a). c) Yield of dextran synthesized in meso and in bulk solution. d) Normalized kinetic curves of sucrose, fructose, and glucose during the reaction. For (b) and (c): mean data with standard deviation error bands and error bars are shown for three independent samples. Synthesis conditions for the in meso reaction: 70 wt% monolinolein and 30 wt% buffer containing 50 mg/mL sucrose and 1 U/mL enzyme at 30°C; for the reaction in bulk solution: 100% buffer containing 50 mg/mL sucrose and 1 U/mL enzyme at 30°C.

meso reaction in Figure 2a for the time points 1 and 2 h. After 24 h, a similar yield of 70% was obtained in both reactions, which, given the difference in M_w after 24 h, suggests that the enzyme immobilized in the mesophase produced a smaller amount of longer polymer chains.

The yield of 70% raised the question of whether the enzyme was unable to convert all the available sucrose. The kinetic curves (Figure 2d) revealed that sucrose was completely depleted after 3 h, implying that the enzyme incorporated glycosyl units into oligosaccharides and sucrose isomers[36] that were washed out during the purification step (Figure S3 and S4). Moreover, the kinetic curves showed a similar progression of sucrose, fructose, and glucose over time between mesophase and bulk solution, with fructose release rates during the major reaction phase between 20 min and 3 h of 0.68 and 0.73 µmol/mL/min in meso and bulk solution, respectively (Figure S5). The specific activity of the enzyme was ≈30 µmol/mg-protein/min in both systems. The kinetic data demonstrated that the enzyme immobilized in lipid mesophase experienced no limitations in terms of substrate accessibility, retained its active conformation, and showed high transglucosylase activity. Indeed, high transglucosylase activity means that the enzyme in the mesophase performs only a very limited hydrolysis reaction, like in bulk solution,[36] which is revealed by the low glucose content in both systems. As such, we hypothesized that the lipid mesophase nanoconfinement, and hence the dimension of the water channels, plays a

crucial role in the observed higher efficiency of in meso enzymatic polymerization.

Water channel diameter influences the molecular weight of in meso synthesized dextran

To confirm this hypothesis, we systematically varied the hydration level of the mesophase between 28 and 34 wt% and determined the M_w of the synthesized dextran. With increasing hydration levels, we observed a clear trend towards lower M_w (Figure 3a). While the dextran synthesized in meso with 72 wt% monolinolein-28 wt% buffer (M72-B28) and M70-B30 showed a unimodal distribution, a bimodal distribution ($Đ = 2.3$) was detected in M66-B34, suggesting that the lower M_w fraction represents dextran synthesized in excess bulk water. Indeed, above a water content of approximately 35 wt% at 30°C, the system of pure monolinolein and water enters the excess water regime,[19] where the mesophase exists at thermodynamic equilibrium with surrounding water.[41]

To obtain a more comprehensive insight into the symmetry of the mesophases and to determine the water channel diameter, we acquired the SAXS profiles of the three mesophase samples with varying hydration levels (Figure 3b). For M72-B28 and M66-B34, the system remained in the *Ia3d* and *Pn3m* phases, respectively, during in meso dextran synthesis, whereas for M70-B30 the mixed *Ia3d + Pn3m* appeared after 24 h. Furthermore, the SAXS profiles of M72-B28 and M66-B34 shifted to higher q-values after 24 h, indicating a decrease in lattice size. These findings are consistent with the observed phase transition to a mixed *Ia3d + Pn3m* phase in M70-B30 after 24 h and can be attributed to the previously mentioned water-binding properties of in meso synthesized dextran.

The water channel diameter in the mesophase (D_{water}) can be calculated directly from the SAXS data and is shown

in Figure 3c. An increase in D_{water} from 2.9 to 3.2 and 3.5 nm with an increase in hydration level from 28 to 30 and 34 wt%, respectively, revealed that the M_w of synthesized dextran is inversely correlated with D_{water}, with longer polymer chains synthesized in smaller water channels. The above results not only complete the picture of induced changes in the mesophase structure during in meso dextran synthesis but also strongly support our hypothesis that the physical diameter of mesophase water channels, i.e., the level of nanoconfinement, directly affects the polymer molecular weight of the dextran synthesized in meso.

Hypothesis on the enzyme working mechanism under soft nanoconfinement

Taken together, our results provide a foundation for interpreting the influence of soft lipidic mesophase nanoconfinement on *DSR-M*-catalyzed dextran synthesis (Figure 4). In bulk solution, *DSR-M* adopts a purely distributive synthesis mechanism in which growing dextran chains are systematically released into the free medium after the addition of a glycosyl unit.[36] Productive encounters between nascent chains and enzymes are thus governed purely by Fickian diffusion in dilute solution. In contrast, with the enzyme immobilized in lipidic mesophase, the diffusion of dextran chains is impeded by the nanoconfined domains of the mesophase. For the *Ia3d* and *Pn3m* phases encountered in this work, theoretical and experimental data have shown that confined polymers experience reduced diffusion compared to bulk aqueous solution, with so-called bottlenecks representing the largest geometric constriction.[18,42] Indeed, when studied in a comparable mesophase system with a water channel diameter of 3.8 nm,[43] dextran polymers of 10 kDa were found to be highly restricted in diffusion compared to bulk diffusion, by about one order of magnitude. We propose that the restricted diffusion of
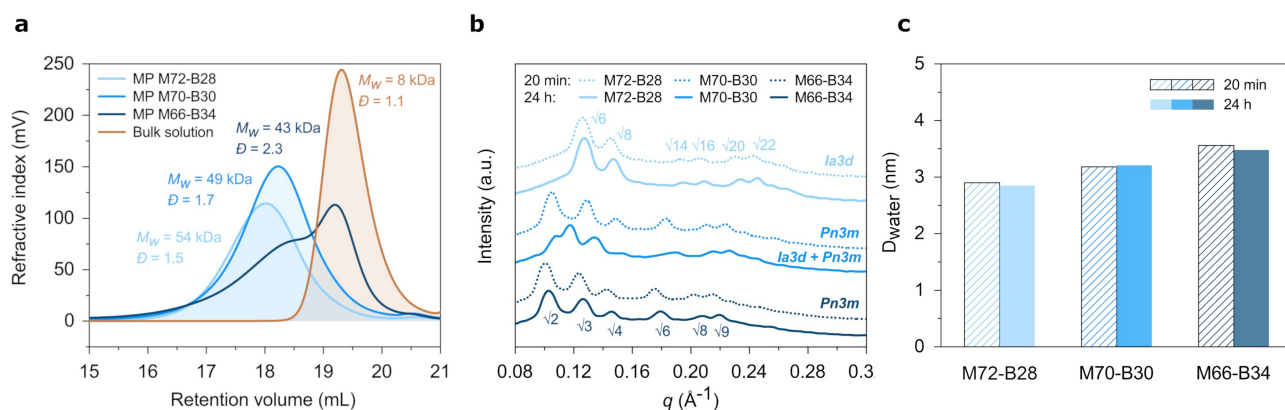

Figure 3. Dextran synthesis in meso with varying hydration levels. a, b) HPSEC profiles of dextran synthesized after 24 h in meso (MP) with varying buffer content of 28, 30, and 34 wt% as compared to dextran synthesized after 24 h in bulk solution (a) and corresponding SAXS profiles of the three mesophase samples 20 min and 24 h after reaction initiation (b). The relative q-values of the Bragg peak positions are included in the SAXS profiles. c) Water channel diameter (D_{water}) in the three mesophase samples with varying buffer content. Synthesis conditions for in meso reactions: Mx-By refers to a mesophase composed of x wt% monolinolein and y wt% buffer containing 50 mg/mL sucrose and 1 U/mL enzyme at 30°C; for the reaction in bulk solution: 100% buffer containing 50 mg/mL sucrose and 1 U/mL enzyme at 30°C. M_w, molecular weight; $Đ$, dispersity; a.u., arbitrary units; q, modulus of scattering vector.
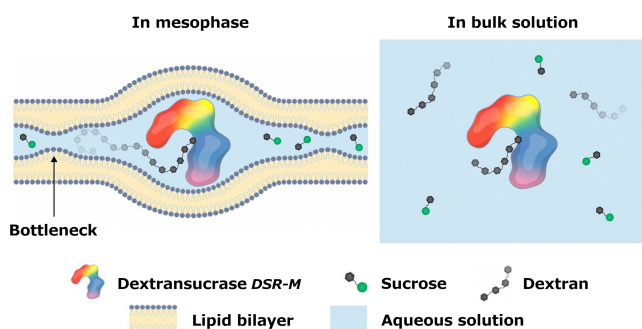
Figure 4. Influence of soft nanoconfinement mediated by lipidic mesophases on the working mechanism of the enzyme dextransucrase *DSR-M*, showing the enzyme embedded between lipid bilayers of the mesophase (left) as compared to the bulk solution (right). The U-shaped enzyme is divided into five domains: red, glucan binding *domain V*; yellow, *domain IV*; green, *domain B*; blue, active site *domain A*; and magenta, *domain C*. For a detailed explanation of the structural domains of *DSR-M*, the reader is referred to Claverie et al.[36]

confined dextran polymers favors the binding of nascent dextran chains to the glucan binding domain (*domain V*, shown in red in Figure 4) of the *DSR-M* enzyme immobilized in the mesophase and induces a shift from a purely distributive to a more processive synthesis mechanism.[36]

In addition, we suspect that the soft nanoconfinement modifies the functional interplay between *domain V*, which undergoes conformational changes during catalytic activity, and the active site of the enzyme (*domain A*, shown in blue in Figure 4), promoting closer proximity among them and further influencing the size of the synthesized polymer.[36,44] This explains well the presence of high M_w dextrans at a very early stage of synthesis, the higher turnover rate after 2–3 h, and the overall higher M_w ($M_w = 49$ kDa) of the in meso synthesized polymers after 24 h compared to the bulk solution ($M_w = 8$ kDa). When we varied the dimension of

the water channel in the mesophase, the observed change in M_w of dextran can be elucidated similarly: a chain will experience a higher probability of a productive encounter with the same enzyme with a stronger confinement effect on diffusion due to smaller water channels.

Enzymatic dextran synthesis at subzero temperature

Inspired by the recent emergence of lipidic mesophases as a platform for subzero chemical reactions,[33,34] we tested whether the enzymatic polymerization of dextran catalyzed by *DSR-M* can be carried out at subzero temperatures. To form the mesophase, we used 91 wt % phytantriol and 9 wt % aqueous phase, since water remains liquid in phytantriol-based mesophases down to $-120\,°C$ below a water content of 9.5 wt %.[33] Remarkably, the in meso immobilized enzyme did synthesize dextran polymers ($M_w = 6$ kDa) at $-20\,°C$, whereas no activity was observed for the reaction in the bulk solution sample (Figure 5a and S6). The reaction time of two months not only attests that subzero temperatures significantly slow down enzymatic reactions, but also that the lifetime of enzymes can be prolonged under these conditions.[45] Isothermal DSC measurements confirmed that the reaction in bulk solution froze at $-20\,°C$ after annealing for 1 h, whereas no ice melting peak was observed for the in meso reaction system (Figure 5b). SAXS measurements showed that the mesophase maintained a lamellar L_α phase over two months, with an approximate distance of 1 nm between the lipid bilayers (Figure 5c and S7). In the L_α phase, the lipid bilayers are able to slide along each other, creating a more dynamic environment in which the enzyme is not completely immobilized, in contrast to the cubic phase. We believe that the fluid nature of the L_α phase combined with the slower diffusion of liquid water at $-20\,°C$[46] were ultimately responsible for the M_w of 6 kDa compared to the observed M_w of 49 kDa for dextran
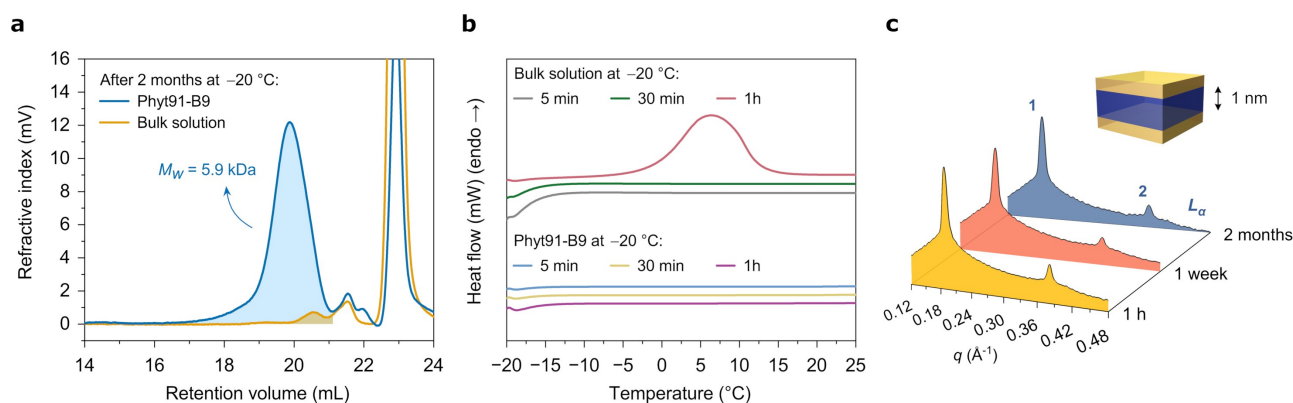

Figure 5. Enzymatic dextran synthesis at subzero temperature. a) HPSEC profiles of dextran synthesized at $-20\,°C$ in Phyt91-B9 and in bulk solution. Note that a peak for dextran is only visible for the in meso reaction. b) DSC melting curves of Phyt91-B9 and bulk solution obtained after annealing at $-20\,°C$ for the times indicated. c) SAXS profile for Phyt91-B9 over 2 months. The relative q-values of the Bragg peak positions are included in the SAXS profiles. Inset: Structure of the lamellar L_α phase with indicated thickness of the water layer. Synthesis conditions for the in meso reaction: 91 wt % phytantriol and 9 wt % buffer (Phyt91-B9) containing 50 mg/mL sucrose and 1 U/mL enzyme at $-20\,°C$; for the reaction in bulk solution: 100 % buffer containing 50 mg/mL sucrose and 1 U/mL enzyme at $-20\,°C$; M_w, molecular weight; a.u., arbitrary units; q, modulus of scattering vector.

synthesized in meso at 30°C. Succinctly summarized, we have used enzymatic dextran synthesis to demonstrate that the synthesis temperature for enzymatic polymerization can be extended into the negative Celsius territory when carried out in meso.

Conclusion

We have demonstrated that lipidic mesophase soft nano-confinement can expand the landscape of enzymatic polymerization in water by providing higher efficiency and a broader operating temperature range. We believe that our findings go beyond the *DSR-M*-catalyzed synthesis of dextran and may bear general significance, at least for in meso enzymatic synthesis of hydrophilic polymer chains and for in meso confined hydrophilic enzymes with similar characteristics, such as low substrate binding affinity. The observed direct dependence of the synthesized polymer molecular weight on the water channel diameter implies prospects for controlling the length of polymers by adjustment of the nanoconfinement level, which should be critically investigated in future work. We envision that our findings may promote readily accessible lipidic mesophases as a biotechnological toolbox to deepen our understanding of the effect of soft nanoconfinement on biochemical reactions. More importantly, these results may open unexplored avenues in the enzymatic synthesis of polymers under ambient and subzero conditions as an alternative to more established synthetic routes for petroleum-based polymers, expanding the scope of polymer synthesis from fundamental to applied sciences and technology.

Conflict of Interest

The authors declare no conflict of interest.

Data Availability Statement

The data that support the findings of this study are available from the corresponding author upon reasonable request.

[1] P. L. Urban, *New J. Chem.* **2014**, *38*, 5135–5141.
[2] H. G. Hansma, *Origins Life Evol. Biospheres* **2014**, *44*, 307–311.
[3] A. B. Grommet, M. Feller, R. Klajn, *Nat. Nanotechnol.* **2020**, *15*, 256–271.
[4] N. Punekar, *ENZYMES: Catalysis, Kinetics and Mechanisms*, Springer, New York, **2018**.
[5] B. Alberts, A. Johnson, J. Lewis, P. Walter, M. Raff, K. Roberts, *Molecular Biology of the Cell 4th Edition: International Student Edition*, Routledge, Oxfordshire, **2002**.
[6] J. Kunkel, P. Asuri, *PLoS One* **2014**, *9*, e86785.
[7] C. M. Agapakis, P. M. Boyle, P. A. Silver, *Nat. Chem. Biol.* **2012**, *8*, 527–535.
[8] A. H. Chen, P. A. Silver, *Trends Cell Biol.* **2012**, *22*, 662–670.
[9] A. Kuchler, M. Yoshimoto, S. Luginbuhl, F. Mavelli, P. Walde, *Nat. Nanotechnol.* **2016**, *11*, 409–420.
[10] D. L. Purich, *Enzyme Kinetics: Catalysis and Control*, Elsevier, Amsterdam, **2010**.
[11] T. E. Sintra, S. P. M. Ventura, J. A. P. Coutinho, *J. Mol. Catal. B* **2014**, *107*, 140–151.
[12] A. Saha, G. Mondal, A. Biswas, I. Chakraborty, B. Jana, S. Ghosh, *Chem. Commun.* **2013**, *49*, 6119–6121.
[13] J. Xie, Q. Shen, K. X. Huang, T. Y. Zheng, L. T. Cheng, Z. Zhang, Y. Yu, G. J. Liao, X. Y. Wang, C. Li, *ACS Nano* **2019**, *13*, 5268–5277.
[14] F. Moyano, R. D. Falcone, J. C. Mejuto, J. J. Silber, N. M. Correa, *Chem. Eur. J.* **2010**, *16*, 8887–8893.
[15] R. Biswas, A. R. Das, T. Pradhan, D. Touraud, W. Kunz, S. Mahiuddin, *J. Phys. Chem. B* **2008**, *112*, 6620–6628.
[16] M. F. Ruiz-Lopez, J. S. Francisco, M. T. C. Martins-Costa, J. M. Anglada, *Nat. Chem. Rev.* **2020**, *4*, 459–475.
[17] S. Kobayashi, H. Uyama, S. Kimura, *Chem. Rev.* **2001**, *101*, 3793–3818.
[18] S. Assenza, R. Mezzenga, *J. Chem. Phys.* **2018**, *148*, 054902.
[19] S. Aleandri, R. Mezzenga, *Phys. Today* **2020**, *73*, 38–44.
[20] P. Ferri, C. Li, D. Schwalbe-Koda, M. Xie, M. Moliner, R. Gómez-Bombarelli, M. Boronat, A. Corma, *Nat. Commun.* **2023**, *14*, 2878.
[21] L. S. Manni, W. K. Fong, R. Mezzenga, *Nanoscale Horiz.* **2020**, *5*, 914–927.
[22] W. J. Sun, J. J. Vallooran, W. K. Fong, R. Mezzenga, *J. Phys. Chem. Lett.* **2016**, *7*, 1507–1512.
[23] C. Speziale, L. S. Manni, C. Manatschal, E. M. Landau, R. Mezzenga, *Proc. Natl. Acad. Sci. USA* **2016**, *113*, 7491–7496.
[24] C. Speziale, A. F. Zabara, C. J. Drummond, R. Mezzenga, *ACS Nano* **2017**, *11*, 11687–11693.
[25] M. Rakotoarisoa, B. Angelov, S. Espinoza, K. Khakurel, T. Bizien, A. Angelova, *Molecules* **2019**, *24*, 3058.
[26] C. E. Conn, C. J. Drummond, *Soft Matter* **2013**, *9*, 3449–3464.
[27] W. J. Sun, J. J. Vallooran, R. Mezzenga, *Langmuir* **2015**, *31*, 4558–4565.
[28] J. J. Vallooran, S. Handschin, S. M. Pillai, B. N. Vetter, S. Rusch, H. P. Beck, R. Mezzenga, *Adv. Funct. Mater.* **2016**, *26*, 181–190.
[29] E. Nazaruk, E. Gorecka, R. Bilewicz, *J. Colloid Interface Sci.* **2012**, *385*, 130–136.
[30] T. Zhou, J. J. Vallooran, S. Assenza, A. Szekrenyi, P. Clapes, R. Mezzenga, *ACS Catal.* **2018**, *8*, 5810–5815.
[31] T. Zhou, J. J. Vallooran, R. Mezzenga, *Nanoscale* **2019**, *11*, 5891–5895.
[32] L. S. Manni, S. Assenza, M. Duss, J. J. Vallooran, F. Juranyi, S. Jurt, O. Zerbe, E. M. Landau, R. Mezzenga, *Nat. Nanotechnol.* **2019**, *14*, 609–615.

[33] Y. Yao, T. Zhou, R. Farber, U. Grossner, G. Floudas, R. Mezzenga, *Nat. Nanotechnol.* **2021**, *16*, 802–810.

[34] T. Zhou, Y. Yao, Q. Zhang, R. Mezzenga, *Chem. Commun.* **2021**, *57*, 5650–5653.

[35] C. Gerday, in *Adaptation and Evolution in Marine Environments, Volume 2* (Eds.: C. Verde, G. di Prisco), Springer, Heidelberg, **2012**, pp. 89–110.

[36] M. Claverie, G. Cioci, M. Vuillemin, N. Monties, P. Roblin, G. Lippens, M. Remaud-Simeon, C. Moulis, *ACS Catal.* **2017**, *7*, 7106–7119.

[37] R. Mezzenga, C. Meyer, C. Servais, A. I. Romoscanu, L. Sagalowicz, R. C. Hayward, *Langmuir* **2005**, *21*, 3322–3333.

[38] Annu, S. Ahmed, in *Advanced Green Materials* (Ed.: S. Ahmed), Woodhead Publishing, **2021**, pp. 1–13.

[39] Y. Yao, S. Catalini, B. Kutus, J. Hunger, P. Foggi, R. Mezzenga, *Angew. Chem. Int. Ed.* **2021**, *60*, 25274–25280.

[40] R. A. Wahab, N. Elias, F. Abdullah, S. K. Ghoshal, *React. Funct. Polym.* **2020**, *152*, 104613.

[41] A. Zabara, R. Mezzenga, *J. Controlled Release* **2014**, *188*, 31–43.

[42] R. Mezzenga, M. Grigorov, Z. D. Zhang, C. Servais, L. Sagalowicz, A. I. Romoscanu, V. Khanna, C. Meyer, *Langmuir* **2005**, *21*, 6165–6169.

[43] R. Negrini, R. Mezzenga, *Langmuir* **2012**, *28*, 16455–16462.

[44] M. Claverie, G. Cioci, M. Guionnet, J. Schorghuber, R. Lichtenecker, C. Moulis, M. Remaud-Simeon, G. Lippens, *Biochemistry* **2019**, *58*, 2853–2859.

[45] A. Jonsson, P. Adlercreutz, B. Mattiasson, *Biotechnol. Bioeng.* **1995**, *46*, 429–436.

[46] W. S. Price, H. Ide, Y. Arata, *J. Phys. Chem. A* **1999**, *103*, 448–450.

[47] D. C. Turner, Z. G. Wang, S. M. Gruner, D. A. Mannock, R. N. Mcelhaney, *J. Phys. II* **1992**, *2*, 2039–2063.

[48] D. M. Anderson, S. M. Gruner, S. Leibler, *Proc. Natl. Acad. Sci. USA* **1988**, *85*, 5364–5368.

[49] J. Briggs, M. Caffrey, *Biophys. J.* **1994**, *66*, 1263–1263.